Improving the $\mathcal{H}_\infty$ norm estimate of an active vibration isolation system using local rational models

E. Geerardyn[1], **T. Oomen**[2], **J. Schoukens**[1]
[1] Vrije Universiteit Brussel, Department ELEC,
Pleinlaan 2, 1050 Brussels, Belgium
e-mail: **egon.geerardyn@vub.ac.be**

[2] Technische Universiteit Eindhoven, Dept. of Mechanical Engineering, Control Systems Technology Group, PO Box 513, Building GEM-Z 0.131, 5600 MB Eindhoven, the Netherlands

Abstract
Accurate uncertainty modeling is crucial in robust vibration controller design. A novel uncertainty modeling technique that enhances the estimated $\mathcal{H}_\infty$ norm of the model error based on the frequency response is developed in this paper. The major innovation is the use of the local rational method (LRM), a local parametric modeling method, to address the inter-grid error. Unlike classical frequency response function (FRF)-based methods that typically underestimate the $\mathcal{H}_\infty$ norm, the proposed technique allows to capture sharp resonance phenomena without the need for a user-intensive and time-consuming model selection step. The performance of the method is illustrated on a simulation example and on measurements of an industrial active vibration isolation system (AVIS). It is shown that in a short measurement time, a reliable estimate of the $\mathcal{H}_\infty$ gain can be attained. On the measurement data, a $7.5\,\mathrm{dB}$ improvement of the $\mathcal{H}_\infty$ norm is observed and validated.

1 Introduction

Robustness is of the utmost importance in vibration isolation to ensure that vibrations are not picked up by sensitive equipment, even when the operational conditions change slightly. An important example includes the active vibration isolation system (AVIS), where feedback is used to isolate high-precision equipment from external disturbances by means of skyhook damping [7]. Unfortunately, skyhook damping performance is limited by flexible resonances present at high frequencies. To tackle this, the ensuing model uncertainties can be accounted for in robust controller design as exemplified in [2, 26]. Unfortunately, these approaches can be inaccurate due to their reliance on rough prior assumptions. This can both lead to overly-conservative controllers when the uncertainty is overestimated, and unreliable controllers when the uncertainty is underestimated. In the latter case no performance or stability can be guaranteed, leading to potentially dangerous situations.

In the literature several approaches have been developed to provide accurate model uncertainty bounds.

1. Model validation is available both in time [17] and frequency [22] domain, but this is often overly optimistic [12].
2. Parametric model-error modeling [9] with explicit characterization of bias and variance requires a significant amount of effort and specific know-how from the user, and rely on assumptions that are asymptotic in the data length.
3. Non-parametric approaches exist [23] that evaluate the $\mathcal{H}_\infty$ norm on a discrete frequency grid. In-between the frequency grid, the error can be bounded in a worst-case sense [3], which can lead to

overly conservative estimates [24, Section 9.5.2].

4. Data-driven approaches [14, 25] have been developed that take the inter-grid error into consideration. However, such methods rely on a series of dedicated iterative experiments and are therefore time-consuming.

The latter methods have revealed that such iterative methods obtain much higher estimates than frequency response function (FRF) based ones, which means that intergrid errors are of key importance for estimating the $\mathcal{H}_\infty$ gain.

This paper proposes a method to estimate the $\mathcal{H}_\infty$ gain based on a single general-purpose experiment of limited length. The key novelty is the usage of local parametric models, provided by the local rational method (LRM) [10], and an interpolation strategy for $\mathcal{H}_\infty$ gain estimation. It is illustrated how this $\mathcal{H}_\infty$ estimate relates to the experiment length. The use of LRM in this context offers a practical golden mean between the global parametric approaches and the non-parametric ones.

Contents In Section 2 the problem is formulated and exemplified. Section 3 introduces the methods used: the local polynomial method (LPM), the LRM and how these can be utilized to estimate the $\mathcal{H}_\infty$ gain. The latter part concerns the essence of this paper. The simulation example of Section 2.1.1 is then discussed further in Section 4. The proposed technique is then illustrated on measurement data of an AVIS in Section 5. Finally, conclusions are drawn and future challenges are discussed in Section 6.

2 Problem formulation

To suppress vibrations, we make use of existing robust control synthesis techniques. Such techniques serve to construct a controller that guarantees good performance and stability for a class of plants. This requires the estimation of a nominal plant model $\hat{P}$ and the size of the plant set in terms of a bound on the model-error Δ. The nominal $\hat{P}$ can be determined through first-principles modeling or system identification. Afterwards, a bound on the model error Δ remains to be estimated.

In this paper, we focus on the estimation of the $\mathcal{H}_\infty$ gain of the model-error Δ to this end. The $\mathcal{H}_\infty$ gain is defined as

$$\gamma = \|\Delta\|_\infty \triangleq \sup_\omega |\Delta(\omega)| \tag{1}$$

for single-input single-output (SISO) systems. In robust control design, $\|\Delta\|_\infty$ (or a weighted variant $\|W\Delta V\|_\infty$) is often used as a measure of the size of the model class [11, 21]. Here, we focus on the unweighted form to ease the presentation. Adapting the presented approach for weighting filters W and V, however, is straightforward.

This paper follows a frequency response function (FRF)-based approach to estimate $\|\Delta\|_\infty$. Note that in practical situations, only a limited amount of data is available to perform this estimation. Consequentially the available frequency resolution is limited, which can cause severe underestimates in resonant systems. The aim of this paper is to obtain an accurate estimate of $\|\Delta\|_\infty$ using a limited amount of input/output data obtained during a single generic experiment.

2.1 Set-up

Examine the linear time-invariant (LTI) system representing the model-error in Figure 1. Its excitation signal $u_\Delta(t)$ is assumed known and its output signal $y_\Delta(t) = y_{\Delta 0}(t) + v(t)$ is disturbed by the colored additive noise v. This system is observed during N samples at the time instances $t = nT_\mathrm{s}$ with $n = 0, 1, \ldots, N-1$ for a sampling time T_s. Using the measured samples of y_Δ and the known samples of u_Δ, we try to recover the FRF of Δ and its peak value $\|\Delta\|_\infty$.

The results for this open-loop set-up can be generalized to closed-loop settings as illustrated in Section 5.

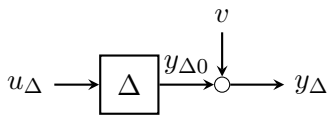

Figure 1: Model-error system Δ in open loop set-up.

2.1.1 Example

Consider the following discrete time system

$$\Delta(z) = \frac{0.454z + 0.448}{z^2 - 1.060z + 0.961} \tag{2}$$

in the set-up depicted in Figure 1 for a sampling time of $T_\mathrm{s} = 1\,\mathrm{s}$. White Gaussian noise $u_\Delta(t)$ with variance $\sigma_u^2 = 1$ is applied at the input. The variance of the noise v is chosen such that the expected signal-to-noise ratio (SNR) at the output is 50 or $34\,\mathrm{dB}$:

$$\mathrm{SNR}_{\text{wanted}} = \|\Delta\|_2 \frac{\sigma_u}{\sigma_v} \approx \frac{\sigma_{y_{\Delta 0}}}{\sigma_v}. \tag{3}$$

After applying N samples of the input sequence and measuring the same amount of output samples, we wish to determine the FRF of Δ. A standard approach to do so is spectral analysis (SA) where he full record of N input/output samples is split into N_S segments of consecutive samples. Each of those N_S segments are then windowed (e.g. using a Hann window) and transformed into the frequency domain by means of the discrete Fourier transform (DFT) (7). Division of the resulting output/input spectra and averaging over the different segments then estimates the FRF of Δ. Alternative approaches to estimate $\Delta(\omega)$, such as the local polynomial method (LPM) and local rational method (LRM), will be introduced in detail in Section 3.

In Figure 2a, an estimate of the FRF of the example Δ (see (2)) is shown by processing the same input/output data record of $N = 97$ samples using:

- spectral analysis (SA) with a Hann window and $N_S = 1$ (i.e. no averaging),
- the local polynomial method (LPM),
- the local rational method (LRM).

It is clear that the limited frequency resolution hampers a good estimation of $\|\Delta\|_\infty$ based on these FRFs. The estimate of $\|\Delta\|_\infty$ using the SA approach cannot be improved by increasing N_S as this would only reduce the frequency resolution. This means that resonances are even more likely to be overlooked.

In this paper, we propose to use locally parametric techniques such as the LPM and LRM to enhance the FRF estimate at the DFT frequency grid on the one hand and gain insight of the inter-grid behavior with the goal of estimating $\|\Delta\|_\infty$. A significant feature of these methods is that the system is not modeled using a global parametric model, thereby avoiding a difficult model selection step.

3 Method: local models

In this section the LPM and LRM are introduced and some practical considerations for their use are given. Starting from the global system equations, the approximations made by the local modeling approaches will be introduced.

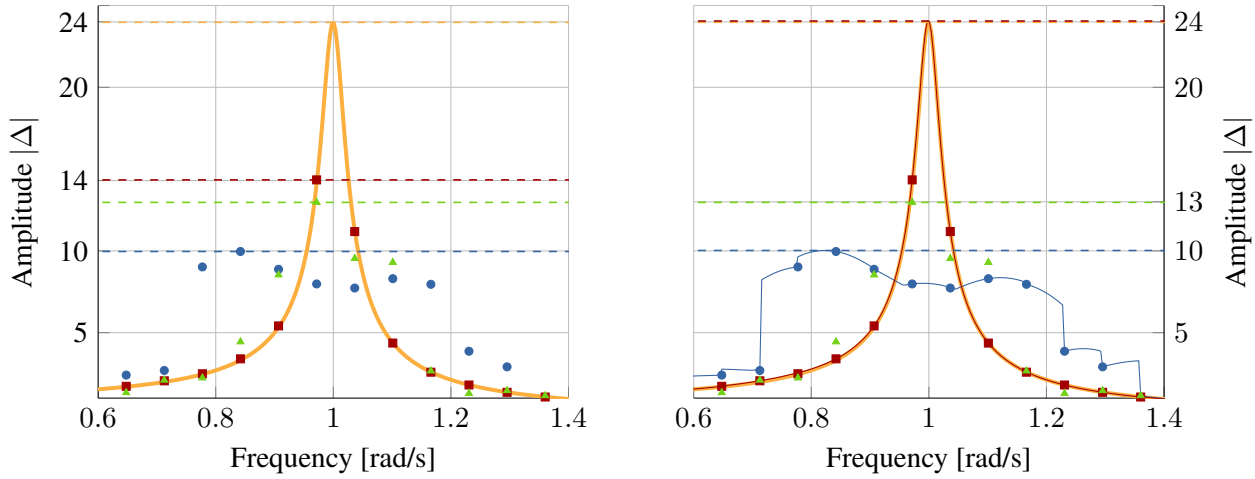

(a) Results without interpolation

(b) Results with interpolation.

Figure 2: Simulation showing that $\|\Delta\|_\infty$(- - -) is underestimated significantly at the discrete frequency grid. The LPM (•), LRM (▪) and SA (▲) estimates of the FRF at the frequency grid are shown together with the true transfer function $\Delta(z)$ (——). These yield under-estimates of the $\mathcal{H}_\infty$ gain of Δ, based on the LPM (- - -), LRM (- - -) and SA (- - -) as shown in Figure 2a. The LPM is severely biased due to the limited frequency resolution. Figure 2b shows that the LRM-interpolation (——) approach proposed in this paper, almost coincides with the true $\Delta(z)$ (——) and correctly estimates the $\mathcal{H}_\infty$ gain (- - -).

For an infinite data length, the system in Figure 1 can be described by

$$y_\Delta(n) = \Delta(z)u_\Delta(n) + v(n) = \Delta(z)u_\Delta(n) + H(z)e(n), \tag{4}$$

where $n = \frac{t}{T_\mathrm{s}}$ is the time normalized by the sampling time T_s, z^{-1} is the lag operator and both $\Delta(z)$ and $H(z)$ are rational functions that are stable and causal. In practice the data length is limited by the measurement time T_m, such that only the samples for $n \in \{0, \ldots, N-1\}$ are obtained. This can be incorporated into (4) by adding the term $t_\Delta(n)$ due to the transient response of the system Δ and, in lesser extent, the noise filter H):

$$y_\Delta(n) = \Delta(z)u_\Delta(n) + t_\Delta(n) + v(n). \tag{5}$$

A relationship equivalent to (5) can be written in the frequency domain, where we denote k as the frequency bin corresponding to $\omega_k = \frac{2\pi k}{NT_\mathrm{s}}$. This results in

$$Y_\Delta(k) = \Delta(\omega_k)U_\Delta(k) + \mathrm{T}_\Delta(\omega_k) + V(k) \tag{6}$$

by transforming (5) using the DFT:

$$X(k) = \frac{1}{\sqrt{N}} \sum_{n=0}^{N-1} x(n) \exp\left(\frac{-j2\pi kn}{N}\right). \tag{7}$$

The local modeling approaches such as the LPM and LRM hinge on the fact that the transfer function $\Delta(\omega)$ and transient $T(\omega)$ are smooth functions over the frequency. This is exploited by describing them using a local (parametric) model. For each frequency ω_k, its local model is estimated by fitting the local model to the input/output data observed at ω_k at a small number of adjacent frequency bins.

3.1 The local polynomial method (LPM)

Smoothness is the underlying principle of the LPM. In (5), both the transfer function $\Delta(\omega_k)$ and the leakage term $T_\Delta(\omega_k)$ are known to be smooth functions in the frequency domain [19].

In the LPM, this smoothness is captured by means of a polynomial series around each frequency bin ω_k:

$$\Delta(\omega_{k+r}) \approx b_0(k) + \sum_{i=1}^{N_B} b_i(k) r^i \triangleq \widetilde{\Delta}_k(r) \tag{8}$$

$$T_\Delta(\omega_{k+r}) \approx t_0(k) + \sum_{i=1}^{N_T} t_i(k) r^i \triangleq \widetilde{T}_k(r) \tag{9}$$

such that $\widetilde{\Delta}_k(r)$ and $\widetilde{T}_k(r)$ are the local models that describe the transfer function and transient in the vicinity of ω_k. The (complex-valued) parameters $b_i(k)$ and $t_j(k)$ are then estimated by considering a local window of $2N_W + 1$ bins around each ω_k such that $r \in \{-N_W, \ldots, +N_W\}$. For this local window, (8) and (9) are substituted in (6) which is fitted in a least-squares sense. This is equivalent to minimizing the following local cost function

$$\sum_{r=-N_W}^{N_W} \left| Y_\Delta(k+r) - \widetilde{\Delta}_k(r) U_\Delta(k+r) - \widetilde{T}_k(r) \right|^2 \tag{10}$$

for each measured frequency ω_k. We denote the LPM applied with above settings as $\mathrm{LPM}\,(N_W, N_B, N_T)$ for brevity.

Note that although we introduce the LPM in a SISO output error (OE) setting, it can be extended to a mutiple-input mutiple-output (MIMO) errors-in-variables (EIV) setting as shown in [15,16]. For more details regarding the LPM, we also refer to [5, 18, 20].

3.2 The local rational method (LRM)

The LRM builds upon the same basic idea as the LPM: locally exploit the structure of the transfer function $\Delta(\omega)$ and leakage $T_\Delta(\omega)$ in the frequency domain [10]. The LRM uses rational functions to capture this behavior:

$$\Delta(\omega_{k+r}) \approx \frac{\sum_{i=0}^{N_B} b_i(k) r^i}{1 + \sum_{i=1}^{N_A} a_i(k) r^i} = \frac{B_k(r)}{A_k(r)} \triangleq \widetilde{\Delta}_k(r) \tag{11}$$

$$T_\Delta(\omega_{k+r}) \approx \frac{\sum_{i=0}^{N_T} t_i(k) r^i}{1 + \sum_{i=1}^{N_A} a_i(k) r^i} = \frac{T_k(r)}{A_k(r)} \triangleq \widetilde{T}_k(r). \tag{12}$$

To estimate the (complex-valued) local parameters $a_i(k)$, $b_i(k)$ and $t_i(k)$, the local models are again substituted into (6). The local cost function

$$\sum_{r=-N_W}^{N_W} \left| A_k(r) Y_\Delta(k+r) - B_k(r) U_\Delta(k+r) - T_k(r) \right|^2 \tag{13}$$

that is minimized, is linked to the method of [8]. We denote the LRM with above settings briefly as $\mathrm{LRM}\,(N_W, N_B, N_A, N_T)$.

3.3 Practical considerations

In this section, a few practical remarks and general recommendations for the use of the LPM and LRM are given.

- The $\mathrm{LPM}\,(N_W, N_B, N_T)$ is identical to $\mathrm{LRM}\,(N_W, N_B, 0, N_T)$, which means that when no denominator $A_k(r)$ is estimated, the LRM reduces to the regular LPM.

- The LPM/LRM amounts to solving a small linear least-squares problem (10)/(13) for each frequency bin. These are a convex optimization problems for which a closed-form solution exist and for which reliable and fast numerical implementations are widely available.
- In applying these local modeling techniques, one still can still use the settings N_W, N_B, N_A and N_T to tune the performance of the method. In [15] it is argued that $N_T = N_B$ is often a good choice. Moreover, these settings are chosen such that the local optimization problems (10)/(13) are overdetermined. That is, the number of complex degrees of freedom ($2N_W - 1 - N_B - N_A - N_T$) has to remain strictly positive. For the LRM, $N_B = N_A = 1$ is a reasonable choice if one assumes that the FRF in each local window ($2N_W + 1$ bins) is predominantly determined by the behavior of a single pole or zero.
- To separate Δ and T_Δ in (6), one has to impose extra constraints on the input signal. These imply that the input spectrum $U(\omega_k)$ should behave sufficiently 'rough' over all frequencies. Practically, this is the case for random noise and random phase multisines [19].
- In most applications, one is interested in the improved FRF estimate of Δ and/or the transient T_Δ at each frequency bin only. This information is estimated directly by means of the $b_0(k)$ and $t_0(k)$ coefficients. In this paper all estimated parameters $b_i(k)$ and $a_i(k)$ need to be stored for every ω_k to be able to interpolate the FRF in-between the frequency grid.
- Note that at the edges of the frequency grid (where $k \leq N_W$ or $k \geq \frac{N}{2} - N_W$), the local window index r in (13) or (10) becomes invalid. This can be worked-around by using an asymmetric local window in these cases as in [15] or by asserting the periodicity of the DFT over ω as in [10]. In this paper, we disregard such edge cases to facilitate the notations but handle them using the former method in the calculations.

3.4 Local models for $\mathcal{H}_\infty$ estimation

In the previous section, it was shown that the LPM and LRM allow to estimate the FRF of the model-error system Δ where the leakage T_Δ has been suppressed. This is basically achieved by approximating Δ and T_Δ around ω_k by low-order local models $\widetilde{\Delta}_k$ and $\widetilde{T}_k$. In this section, we exploit the local models estimated by the LRM or LPM to gain insight into the inter-grid behavior of Δ and eventually estimate $\|\Delta\|_\infty$.

In a typical FRF-based approach, only a discrete grid of values for ω_k is available. As in [23], the $\mathcal{H}_\infty$ norm is then approximated by:

$$\gamma_{\mathrm{FRF}} \triangleq \max_{\omega_k} |\Delta(\omega_k)| \leq \|\Delta\|_\infty = \gamma \tag{14}$$

where the discrete frequency grid gives rise to an underestimate of γ as shown in Figure 2a.

The main concern is to determine $\Delta(\omega)$ for ω in-between the observed frequency grid. For the LPM/LRM each frequency bin ω_k has an associated local model $\widetilde{\Delta}_k$ that was estimated using input/output data of its surrounding bins. To reinforce this interpretation, we introduce the notation

$$\Delta_k\left(\omega_{k+r}\right) \triangleq \widetilde{\Delta}_k(r) \tag{15}$$

as the frequency response of Δ in ω_{k+r} according to the local model around frequency bin ω_k. For every ω (within the extent of the frequency grid), this means that two adjacent local models can be found: $\Delta_{k_L(\omega)}$ and $\Delta_{k_R(\omega)}$. As these models are parametric (see (11)), they can be evaluated over a continuous frequency range ω around the corresponding frequency bins.

To estimate $|\Delta(\omega)|$ in the definition of the $\mathcal{H}_\infty$ norm (1), this means that the LPM/LRM provides us with two candidate estimates: $\left|\Delta_{k_L(\omega)}(\omega)\right|$ and $\left|\Delta_{k_R(\omega)}(\omega)\right|$. In spirit of the worst-case interpretation of the $\mathcal{H}_\infty$ norm, a pragmatic solution is to retain only the largest of both:

$$|\Delta(\omega)|_{\mathrm{LRM}} = \max\left\{\left|\Delta_{k_L(\omega)}(\omega)\right|, \left|\Delta_{k_R(\omega)}(\omega)\right|\right\}. \tag{16}$$

This naturally leads to an estimate of the $\mathcal{H}_\infty$ gain using local models:

$$\gamma_{\mathrm{LRM}} \triangleq \|\widehat{\Delta_{\mathrm{LRM}}}\|_\infty \triangleq \max_\omega |\Delta(\omega)|_{\mathrm{LRM}} = \max_\omega \max \left\{ \left|\Delta_{k_L(\omega)}(\omega)\right|, \left|\Delta_{k_R(\omega)}(\omega)\right| \right\}. \tag{17}$$

Instead of performing the formal optimization problem (17) over the continuous frequency ω, we approximate its solution by evaluating this expression on a sufficiently dense frequency grid. This approximates the original problem up to arbitrary precision by increasing the grid density of ω.

4 Simulation

We revisit the example given in Section 2.1.1 to examine the performance of the proposed $\mathcal{H}_\infty$ gain estimation procedure (17) . The basic set-up is given in Figure 1 with $\Delta(z)$ defined in (2). The results for methods that only take the on-grid FRF into account have been presented in Figure 2a. It is clear that the limited frequency resolution hampers their usability.

By taking a closer look at the results in Figure 2b of the $\mathrm{LPM}\,(5, 2, 2)$ and $\mathrm{LRM}\,(6, 1, 1, 1)$, we see that the LPM is not well-adapted to this setting. Obviously, the interpolation is not improving the poor performance at the discrete frequency grid for the inter-grid frequencies. Around this resonance, the LPM needs enough points to capture the resonant pole using only the numerator coefficients [20].

The LRM on the other hand performs well in Figure 2b. Both the theoretical value and the interpolated $|\Delta|_{\mathrm{LRM}}$ coincide almost perfectly. The $\mathcal{H}_\infty$ gain obtained using interpolation is equal to the theoretical $\|\Delta\|_\infty = 24$, a huge improvement over the on-grid estimate of $\gamma_{\mathrm{FRF}}^{(\mathrm{LRM})} = 14$. Intuitively, the LRM locally estimates a single (complex) pole to model the resonance, which yields a much better approximation than the LPM. These results indicate that the proposed method is able to retrieve the $\mathcal{H}_\infty$ gain well from simulated input/output data using only a limited number of samples.

4.1 Considerations for the experiment length

It has become apparent that frequency resolution, and hence measurement time, is crucial to obtain a good estimate of the $\mathcal{H}_\infty$ gain. By properly interpolating local models this effect can be mitigated as demonstrated in the previous section. Obviously, there will still be a minimal frequency resolution required to capture the resonant pole using the LRM.

In this section we briefly look into the effect of the record length N (i.e. measurement time) on the estimated $\|\widehat{\Delta_{\mathrm{LRM}}}\|_\infty$. This is done by running the original simulation depicted in Section 2 for a large number of samples. From the simulated input/output data only the first N samples are used to estimate $\|\Delta\|_\infty$ by applying the interpolation approach (17) to both LPM and LRM. For the same large data record, the effective record length N is then varied between 28 and 16000. The corresponding estimates are shown in Figure 3. In practical environments, rules-of-thumb are often used to guess the required measurement time T_{m}. Such rules typically relate measurement time and the dominant time constant τ of the system [20], e.g. $T_{\mathrm{m}} \geq 5\tau$. For the simulated system (2), the time constant $\tau = 50$ samples, which allows us to compare the results of the proposed method with such heuristics.

Figure 3 shows that $N \geq 1000 = 20\tau$ is required to properly estimate the peak amplitude using only the FRF at the discrete frequency grid, even when noiseless data would be available. As expected, for very large values of N, all methods provide an identical estimate that coincides with the true value. The interpolated LRM yields an improved estimate when $N \geq 97 \approx 2\tau$; the LPM is unable to provide such an advantage. This means that in this particular case, the interpolated LRM approach improves over the on-grid estimate using a data record that is ten times shorter.

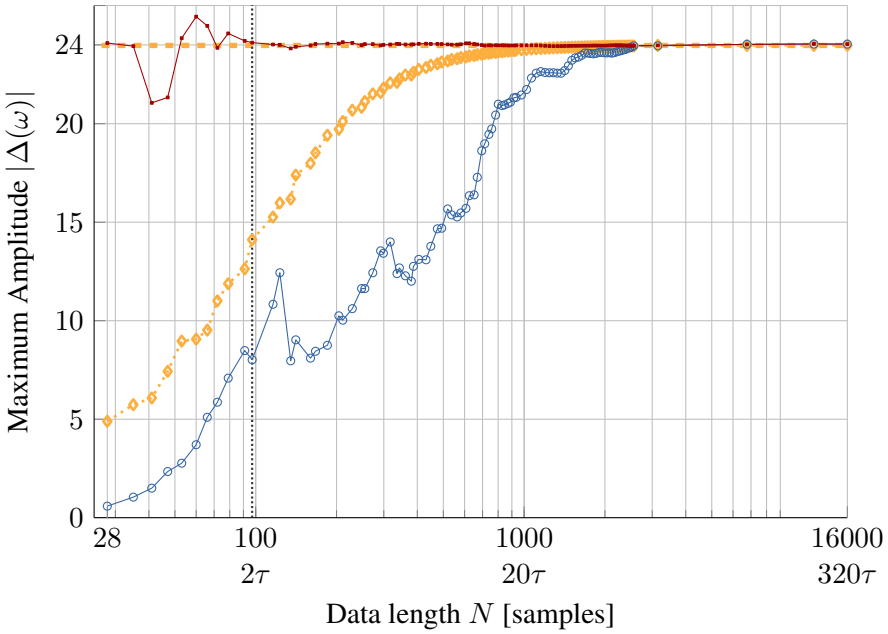

Figure 3: The $\mathcal{H}_\infty$ norm of the true FRF on the discrete frequency grid, γ_{FRF} (···◇···), significantly underestimates the actual $\|\Delta\|_\infty$ (- - -) for short experiments where $N < 1000$. The proposed estimate $\|\widehat{\Delta_{\text{LRM}}}\|_\infty$ (—•—) is already reliable when $N \geq 97$, unlike $\|\widehat{\Delta_{\text{LPM}}}\|_\infty$ (—○—). For $N = 97$ (·····) the obtained FRFs are shown in Figure 2.

5 Experimental verification on an active vibration isolation system

The method proposed in this paper is illustrated on the industrial active vibration isolation system (AVIS) in Figure 4. This AVIS is composed of a support structure affixed to the ground and a payload platform suspended on airmounts such that it can move freely. The active control part of the AVIS consists of six geophones that measure the platform velocity and eight Lorentz motors attached at the corners. To ease the presentation, we only consider a SISO part of this AVIS, particularly the vertical translation.

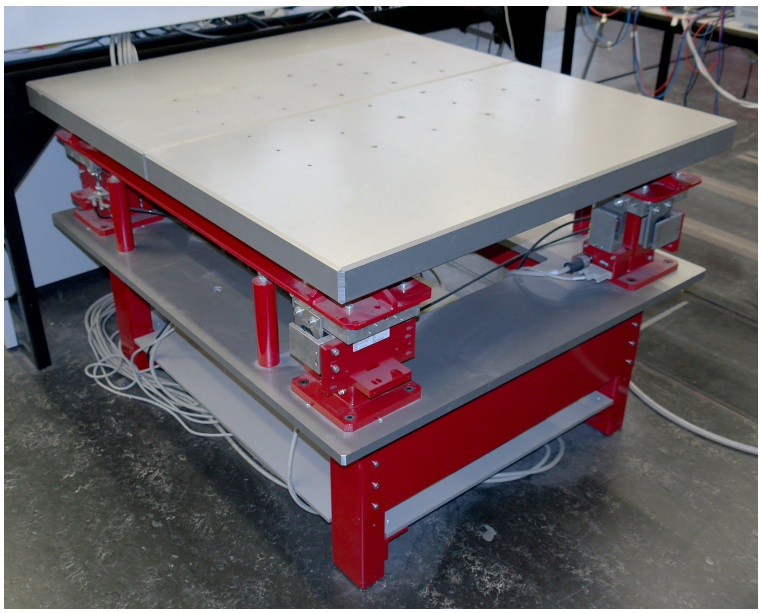

Figure 4: The active vibration isolation system (AVIS).

5.1 Robust control framework

As the AVIS operates in closed-loop, a suitable uncertainty representation is used: the so-called dual-Youla-Kučera structure [1, 6]. This leads to a model set $\mathcal{P}$ shown in Figure 5 and described formally by

$$\mathcal{P} \triangleq \left\{ \left. \frac{\hat{N} + D_c\Delta}{\hat{D} - N_c\Delta} \right| \|\Delta\|_\infty \leq \gamma_\mathcal{P} \right\}, \tag{18}$$

in which $\gamma_\mathcal{P}$ is the $\mathcal{H}_\infty$ norm that is to be estimated. To do so, u_Δ and y_Δ are required in Figure 5. In [1] it is shown that u_Δ can be calculated without any influence of noise but y_Δ is disturbed by noise. Consequentially the dual-Youla structure (Figure 5) simplifies to output-error (Figure 1) regarding the estimation of $\|\Delta\|_\infty$.

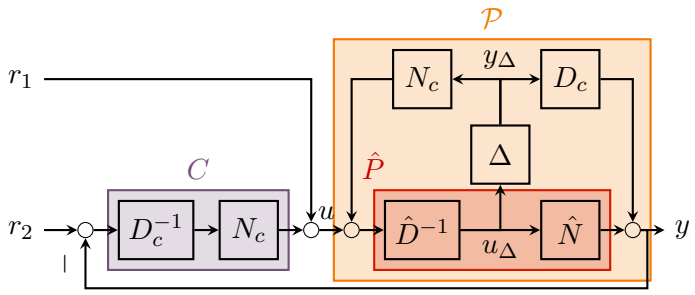

Figure 5: Dual-Youla model structure.

5.2 Measurement results

Beforehand, we determine an eight-order parametric model $\hat{P}$ as a coprime factorization. This is a global parametric model that is fitted using the identification framework of [13] employing the same $\mathcal{H}_\infty$ criterion $\|WT(P, C)V\|_\infty$ for both system identification and robust controller design where $T(P, C)$ denotes the closed-loop transfer function from $\begin{bmatrix} r_1 & r_2 \end{bmatrix}^\mathrm{T}$ to $\begin{bmatrix} u & y \end{bmatrix}^\mathrm{T}$ in Figure 5 and W and V are weighting filters. The estimated model $\hat{P}$ is shown in Figure 6.

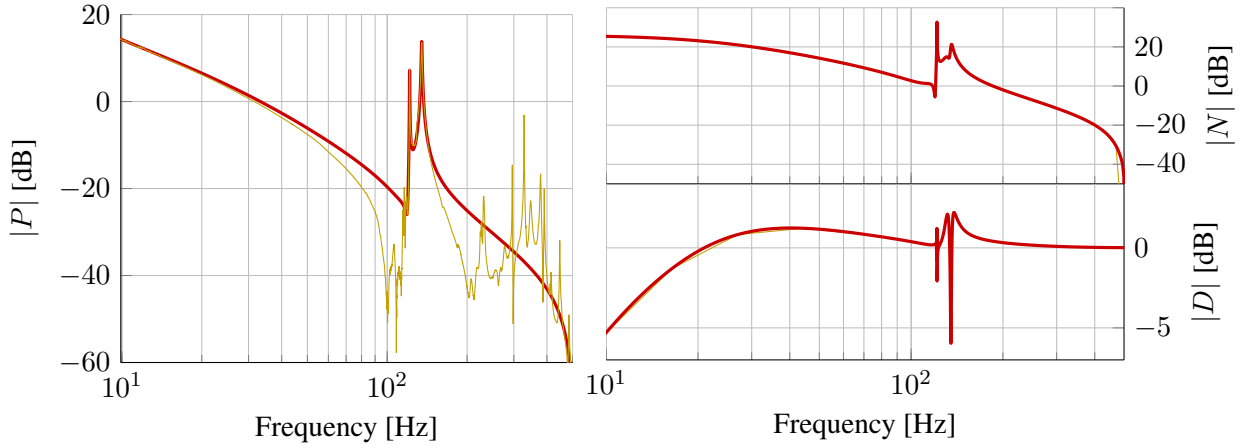

(a) Plant Model $\hat{P} = \hat{N}\hat{D}^{-1}$.

(b) Estimated plant coprime factors $\hat{N}$ and $\hat{D}$.

Figure 6: Estimated parametric model $\hat{P} = \hat{N}\hat{D}^{-1}$ (—■—) of the AVIS and a measured FRF (·····).

We measure the FRF of the AVIS using five periods of a random phase quasi-logarithmic multisine [4]. Each period contains 65 636 samples with a sampling time of $T_\mathrm{s} = 1\,\mathrm{ms}$ and 1550 bins are excited in such a way that $\frac{\omega_k}{\omega_{k-1}} \approx 1.001$. This excitation signal is applied at the feed-forward input r_1, while the set-point

(r_2) is kept zero in the feedback set-up with an experimental PID controller C^{exp} in place. The estimated model (Figure 6) provides a reasonable description of the plant behavior, but obviously doesn't capture all the dynamics. These unmodeled dynamics are then part of Δ, whose FRF is determined [1] by calculating u_Δ and y_Δ from the known controller C^{exp} and estimated nominal plant model $\hat{P}$.

To evaluate the performance of the proposed method on a low-resolution frequency grid, we take one out of every four bins to perform the estimation. We process these bins using $\text{LRM}\,(6, 2, 2, 2)$ and $\text{LPM}\,(4, 2, 2)$ to obtain both the FRF and their interpolated counterparts. To validate these results, the full data record is used and processed using the LRM as shown in Figure 7.

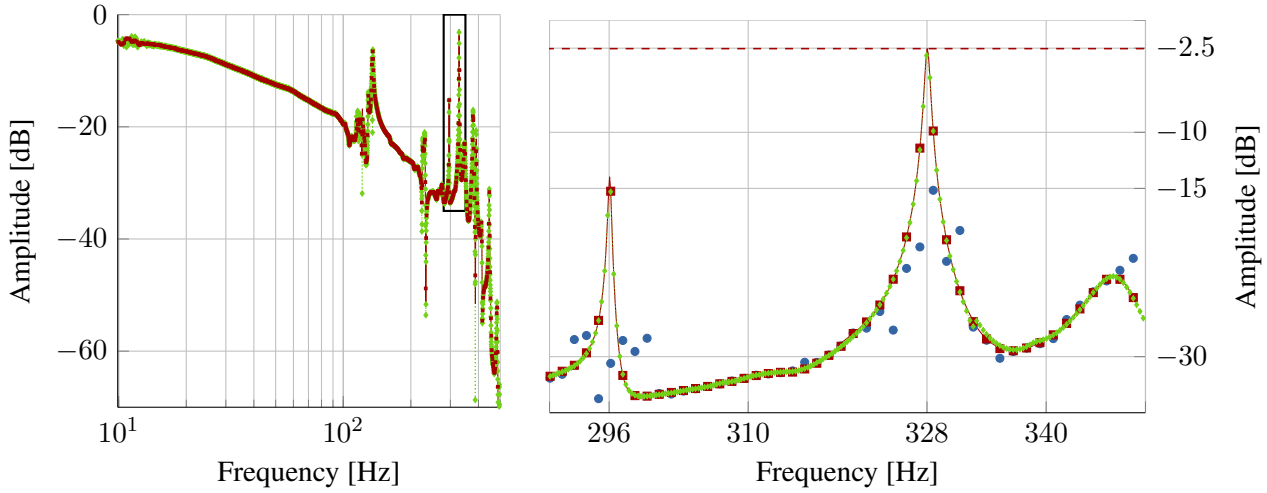

(a) Measured Δ of the AVIS.

(b) Zoomed fragment of Figure 7a.

Figure 7: Measured Δ of the AVIS. The FRF estimated by the LPM (•) and LRM (▪) on a sparse frequency grid is shown. It can be observed that the $\text{LPM}\,(4, 2, 2)$ is unable to properly capture the resonance peaks. By interpolating the LRM (—▪—) the estimate of the peak amplitude near 329 Hz is improved by 7.5 dB. Both the interpolation and the peak estimate are validated against a four times denser data record (·◆·).

In Figure 7 one can observe that the LPM is again unable to properly capture the resonance peaks. The interpolated LRM for the estimation data and validation record agree to about 5%. Moreover, the resonance peak at 328 Hz (Figure 7b) is estimated well using only the sparse frequency grid, but in agreement with the dense validation record. The corresponding peak amplitude of -2.5 dB for the interpolated LRM improves upon the non-interpolated peer by 7.5 dB in amplitude. Again, this is seen to be in good agreement with the four times denser validation data record. This again underlines that the interpolated LRM is able to provide a good estimate of $\|\Delta\|_\infty$ using much less data (or measurement time).

6 Conclusions

Non-conservative robust control design for vibration suppression requires a reliable estimate of the $\mathcal{H}_\infty$ norm of the model error Δ. In this paper, we have presented a novel technique to estimate $\|\Delta\|_\infty$ by interpolating neighboring low-order local parametric models obtained by the LRM. This technique does not depend on a global parametric model, but it takes the inter-grid behavior into account. In this paper it is illustrated on simulations that $\|\Delta\|_\infty$ can be estimated reliably without a difficult model selection step. Moreover, measurement time is reduced by almost an order of magnitude compared to basic FRF-based techniques. The method is validated on measurements of an industrial AVIS where an improvement of 7.5 dB was observed and validated for $\|\Delta\|_\infty$. Ongoing research focuses on extending these results to the MIMO case.

Acknowledgments

This work is supported by the Fund for Scientific Research (FWO-Vlaanderen), by the Flemish Government (Methusalem), by the Belgian Government through the Interuniversity Poles of Attraction (IAP VII-Dysco) Program, and by the Innovational Research Incentives Scheme under the VENI grant *"Precision Motion: Beyond the Nanometer"* (no. 13073) awarded by NWO (Netherlands Organization for Scientific Research) and STW (Dutch Science Foundation).

References

[1] B. D. O. Anderson, *From Youla-Kucera to identification, adaptive and nonlinear control*, Automatica **34** (1998), no. 12, 1485–1506.

[2] Y. Chida, Y. Ishihara, T. Okina, T. Nishimura, K. Ohtomi, and R. Furukawa, *Identification and frequency shaping control of a vibration isolation system*, Control Engineering Practice **16** (2008), no. 6, 711–723.

[3] D. K. de Vries and P. M. J. Van den Hof, *Quantification of model uncertainty from data*, International Journal of Robust and Nonlinear Control **4** (1994), no. 2, 301–319.

[4] E. Geerardyn, Y. Rolain, and J. Schoukens, *Design of quasi-logarithmic multisine excitations for robust broad frequency band measurements*, IEEE Transactions on Instrumentation And Measurements **62** (2013), no. 5, 1364–1372.

[5] M. Gevers, R. Pintelon, and J. Schoukens, *The local polynomial method for nonparametric system identification: improvements and experimentation*, IEEE Conference on Decision and Control and European Control Conference (Orlando, Florida), 2011.

[6] F. Hansen, G. Franklin, and R. Kosut, *Closed-loop identification via the fractional representation: Experiment design*, American Control Conference, 1989, 1989, pp. 1422–1427.

[7] D. Karnopp, *Active and semi-active vibration isolation*, Transactions of the ASME **117** (1995), 177–185.

[8] E. C. Levy, *Complex-curve fitting*, Automatic Control, IRE Transactions on **AC-4** (1959), no. 1, 37–43.

[9] L. Ljung, *Model validation and model error modeling*, The Åström Symposium on Control (Lund, Sweden) (B. Wittenmark and A. Rantzer, eds.), Studentlitteratur, 1999, pp. 15–42.

[10] T. McKelvey and G. Guérin, *Non-parametric frequency response estimation using a local rational model*, Proceedings of the 16th IFAC Symposium on System Identification, July 11-13 (Brussels), July 2012.

[11] T. Oomen and O. Bosgra, *Robust-control-relevant coprime factor identification: A numerically reliable frequency domain approach*, American Control Conference, 2008, june 2008, pp. 625 –631.

[12] ———, *Well-posed model uncertainty estimation by design of validation experiments*, 15th IFAC Symposium on System Identification (Saint-Malo, France), 2009, pp. 1199–1204.

[13] T. Oomen and O. Bosgra, *System identification for achieving robust performance*, Automatica **48** (2012), no. 9, 1975 – 1987.

[14] T. Oomen, R. van der Maas, C.R. Rojas, and H. Hjalmarsson, *Iterative data-driven $\mathcal{H}_\infty$ norm estimation of multivariable systems with application to robust active vibration isolation*, IEEE Transaction on Control Systems Technology **PP** (2014), no. 99, 1–1, Early Access, DOI 10.1109/TCST.2014.2303047.

[15] R. Pintelon, J. Schoukens, G. Vandersteen, and K. Barbé, *Estimation of nonparametric noise and FRF models for multivariable systems – part I: Theory*, Mechanical Systems and Signal Processing **24** (2010), no. 3, 573 – 595.

[16] _____, *Estimation of nonparametric noise and FRF models for multivariable systems – part II: Extensions, applications*, Mechanical Systems and Signal Processing **24** (2010), no. 3, 596 – 616.

[17] K. Poolla, P. Khargonekar, A. Tikku, J. Krause, and K. Nagpal, *A time-domain approach to model validation*, IEEE Transactions on Automatic Control **39** (1994), no. 5, 951–959.

[18] J. Schoukens, Y. Rolain, and R. Pintelon, *Leakage reduction in frequency-response function measurements*, IEEE Transaction on Instrumentation and Measurement **55** (2006), no. 6, 2286 –2291.

[19] J. Schoukens, G. Vandersteen, K. Barbé, and R. Pintelon, *Nonparametric preprocessing in system identification: a powerful tool*, European Journal of Control **15** (2009), no. 3–4, 260 – 274.

[20] J. Schoukens, G. Vandersteen, R. Pintelon, Z. Emedi, and Y. Rolain, *Bounding the polynomial approximation errors of frequency response functions*, IEEE Transaction on Instrumentation and Measurement **62** (2013), no. 5, 1346–1353.

[21] S. Skogestad and I. Postlethwaite, *Multivariable feedback control: analysis and design*, second ed., Wiley, 2005.

[22] R. S. Smith and J. C. Doyle, *Model validation: A connection between robust control and identification*, IEEE Transactions on Automatic Control **37** (1992), no. 7, 942–952.

[23] M. van de Wal, G. van Baars, F. Sperling, and O. Bosgra, *Multivariable $\mathcal{H}_\infty/\mu$ feedback control design for high-precision wafer stage motion*, Control Engineering Practice **10** (2002), no. 7, 739–755.

[24] G. Vinnicombe, *Uncertainty and feedback: $\mathcal{H}_\infty$ loop-shaping and the ν-gap metric*, Imperial College Press, London, United Kingdom, 2001.

[25] B. Wahlberg, M. Barenthin Syberg, and H. Hjalmarsson, *Non-parametric methods for $\mathcal{L}_2$-gain estimation using iterative experiments*, Automatica **46** (2010), no. 8, 1376–1381.

[26] Y. Zhang, A. G. Alleyne, and D. Zheng, *A hybrid control strategy for active vibration isolation with electrohydraulic actuators*, Control Engineering Practice **13** (2005), no. 3, 279–289.